TRENDS in Neurosciences

January 2005
Vol. 28, No. 1
pp. 1–56

Editorial Enquiries
Trends in Neurosciences
Elsevier,
84 Theobald's Road,
London, UK WC1X 8RR
Tel: +44 (0)20 7611 4400
Fax: +44 (0)20 7611 4470
E-mail: tins@elsevier.com

Subscription Enquiries
E-mail: ct.subs@qss-uk.com

Forthcoming articles

Cell transplantation in Parkinson's disease: how can we make it work?
C. Winkler, D. Kirik and A. Bjorklund

Hippocampal sequence encoding driven by a cortical multi-item working memory buffer
O. Jensen and J. Lisman

Memory retention – the synaptic stability versus plasticity dilemma
W.C. Abraham and A. Robins

Multiple facets of GABAergic neurons and synapses: multiple fates of GABA signalling in epilepsies
R. Cossart, C. Bernard and Y. Ben-Ari

Neuropathic pain and spinal microglia: a big problem from molecules in 'small' glia
M. Tsuda, K. Inoue and M.W. Salter

Synaptic mechanisms of the cerebellar cortical network
S. Nakanishi

Similarities between the actions of estrogen and BDNF in the hippocampus: coincidence or clue?
H. Scharfman and N.J. MacLusky

TRENDS
www.trends.com

Cover: A bipolar cell axon terminal (blue) with a presynaptic ribbon (red), bearing a cloud of tethered vesicles, some of which are docked (yellow) at the active zone. This special structure allows a high rate of exocytosis to be sustained, probably because docked vesicles can be released instantaneously upon Ca^{2+} influx and can be rapidly replaced by the tethered vesicles that are 'pre-ripened' for release. Processes include a ganglion cell dendrite and an amacrine process (containing vesicles) that feeds back to the bipolar cell. Peter Sterling and Gary Matthews review the cell biology and physiology of the ribbon synapse in pages 20–29 of this issue.

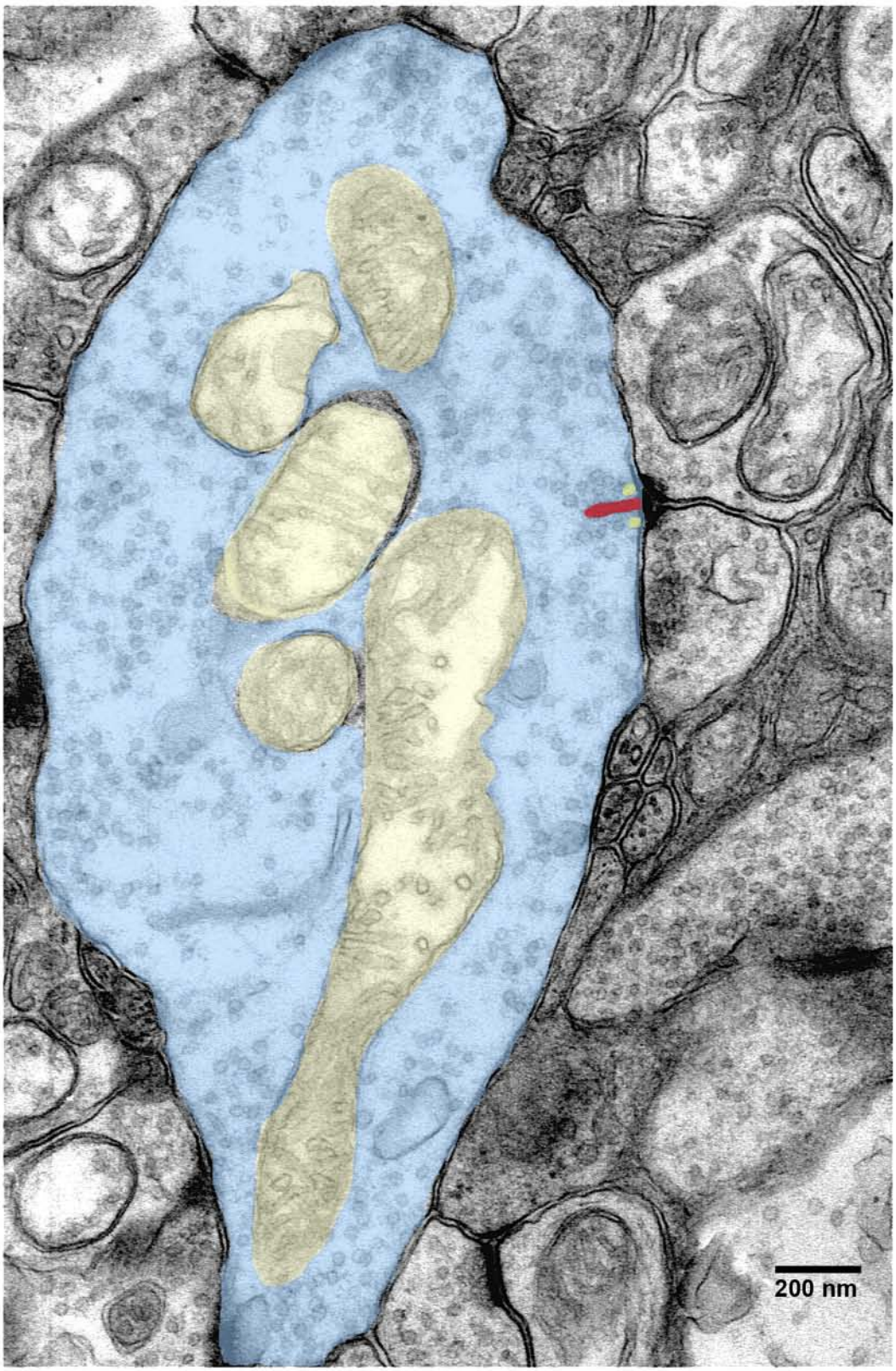
200 nm

Review TRENDS in Neuroscientes Vol.28 No.1 January 2005

Synaptic Connectivity series

Structure and function of ribbon synapses

Peter Sterling[1] and Gary Matthews[2]

[1]Department of Neuroscience, University of Pennsylvania, Philadelphia, PA 19104, USA
[2]Department of Neurobiology, State University of New York, Stony Brook, NY 11794, USA

Sensory neurons with short conduction distances can use nonregenerative, graded potentials to modulate transmitter release continuously. This mechanism can transmit information at much higher rates than spiking. Graded signaling requires a synapse to sustain high rates of exocytosis for relatively long periods, and this capacity is the special virtue of ribbon synapses. Vesicles tethered to the ribbon provide a pool for sustained release that is typically fivefold greater than the docked pool available for fast release. The current article, which is part of the *TINS Synaptic Connectivity* series, reviews recent evidence for this fundamental computational strategy and its underlying cell biology.

The synaptic 'ribbon' is an organelle expressed in the terminals of vertebrate photoreceptors and their second-order neurons (bipolar cells). Ribbons are also expressed by auditory and vestibular hair cells (reviewed in Ref. [1]) and in electrosensory receptors [2]. In fact, the ribbon seems to occur wherever synaptic exocytosis is evoked by graded depolarization and where signaling requires a high rate of sustained release (Figure 1). Ribbon synapses invariably use glutamate as the primary transmitter. The present article summarizes recent progress in understanding the role of this peculiar organelle (see also Refs [3–6]).

Microscopic structure

The photoreceptor ribbon is typically a plate, ~30 nm thick, that extends perpendicular to the plasma membrane (Figures 2 and 3). The ribbon juts ~200 nm into the cytoplasm, and never much more, but can vary in length from 200–1000 nm. The ribbon anchors along its base to an electron-dense structure (arciform density) that in turn anchors to the presynaptic membrane. This allows the ribbon to float ~20 nm above the membrane like a flag or a balloon on a short leash. One puzzle is that hair cells lack an arciform density, so the anchor of the ribbon is invisible by standard electron-microscopic procedures.

The ribbon's surface is studded with small particles (~5 nm diameter) to which synaptic vesicles tether via fine filaments (~5 nm thick and ~40 nm long). Usually there are several filaments per vesicle [7]. Tethered vesicles cluster densely but do not touch. Vesicles tethered along

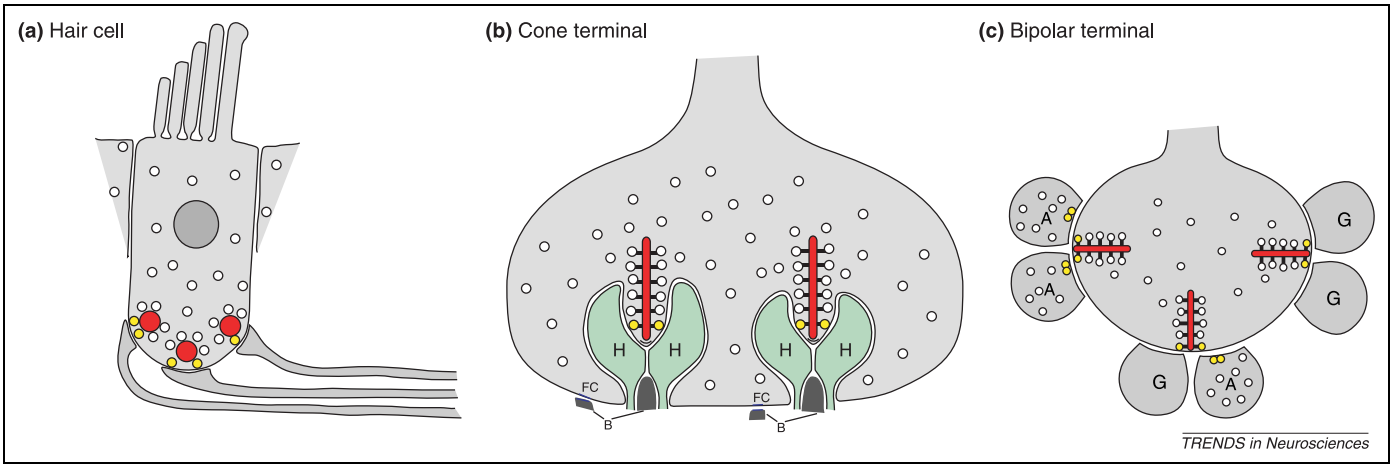

Figure 1. Diversity of ribbon synapses. **(a)** A hair cell. At the apical pole, cilia express the transduction channels. At the basal pole, ribbons (red; also known as 'dense bodies') tether numerous vesicles (white and yellow; the yellow vesicles are docked) near the presynaptic membrane. Each ribbon supplies one postsynaptic process. A hair cell typically contains 10–20 ribbons. **(b)** A cone terminal. Each ribbon (red) is located at the apex of an invagination that accommodates a triad of postsynaptic processes: two lateral processes (horizontal cells, H) and one central process (bipolar dendrite, B). Each cone typically expresses 20–50 triads. Flat contacts (FC) represent a different type of bipolar dendrite (Figure 5a). **(c)** A bipolar terminal. Each ribbon supplies a dyad of postsynaptic processes, which can comprise two ganglion cell dendrites (G), one ganglion cell dendrite and one amacrine process (A), or two amacrine processes. The amacrine processes often return a synapse to the bipolar terminal.

Corresponding author: Sterling, P. (peter@retina.anatomy.upenn.edu).
Available online 2 December 2004

 0166-2236/$ - see front matter doi:10.1016/j.tins.2004.11.009

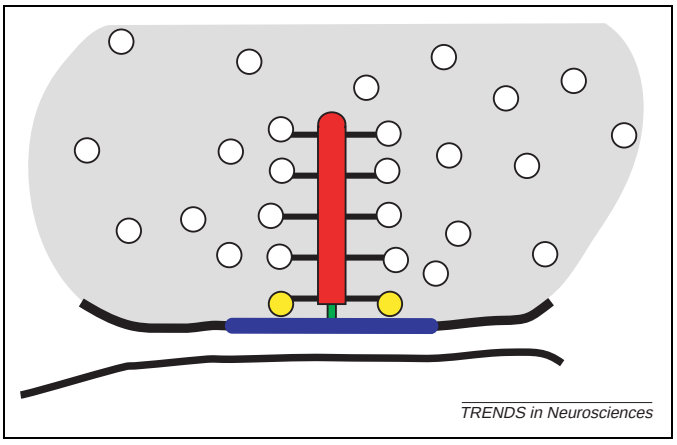

Figure 2. Generic ribbon synapse. The ribbon (red) anchors near presynaptic membrane with the assistance of the protein Bassoon (green), which can also associate with voltage-gated Ca^{2+} channels (blue) that cluster in the underlying plasma membrane. Vesicles that press against the plasma membrane (yellow) are considered 'docked' and correspond to the 'ultrafast' pool; the remaining vesicles tethered to the ribbon correspond to the 'readily releasable pool'. Vesicles unattached to the ribbon diffuse freely in the cytoplasm [19,80].

the base of the ribbon directly contact the presynaptic membrane and thus are considered 'docked'. Consequently, the ribbon's geometry establishes a fixed ratio between the numbers of vesicles tethered and docked, roughly 5:1 for plate-like ribbons and 10:1 for spheroidal ones [8,9]. The space between spherical ribbons and the membrane is occupied by docked synaptic vesicles which, in lieu of an arciform density, might keep the sphere in place.

Molecular structure

Several proteins associated with the ribbon have been identified. First, there is RIM, which is present at all synapses and interacts with rab3, a GTPase expressed on synaptic vesicles [10]. Second, there is RIBEYE, which has a novel A domain at the N terminus and a B domain, identified as the transcriptional suppressor, CtBP2 [11,12]. This domain is homologous to a specific dehydrogenase and might serve enzymatically. CtBP2 has also been localized to hair cell ribbons [12]. Third, there is immunostaining for KIF3A, a kinesin motor [13]. Finally, there are Bassoon and Piccolo, presynaptic 'cytomatrix' proteins, which are also associated with conventional

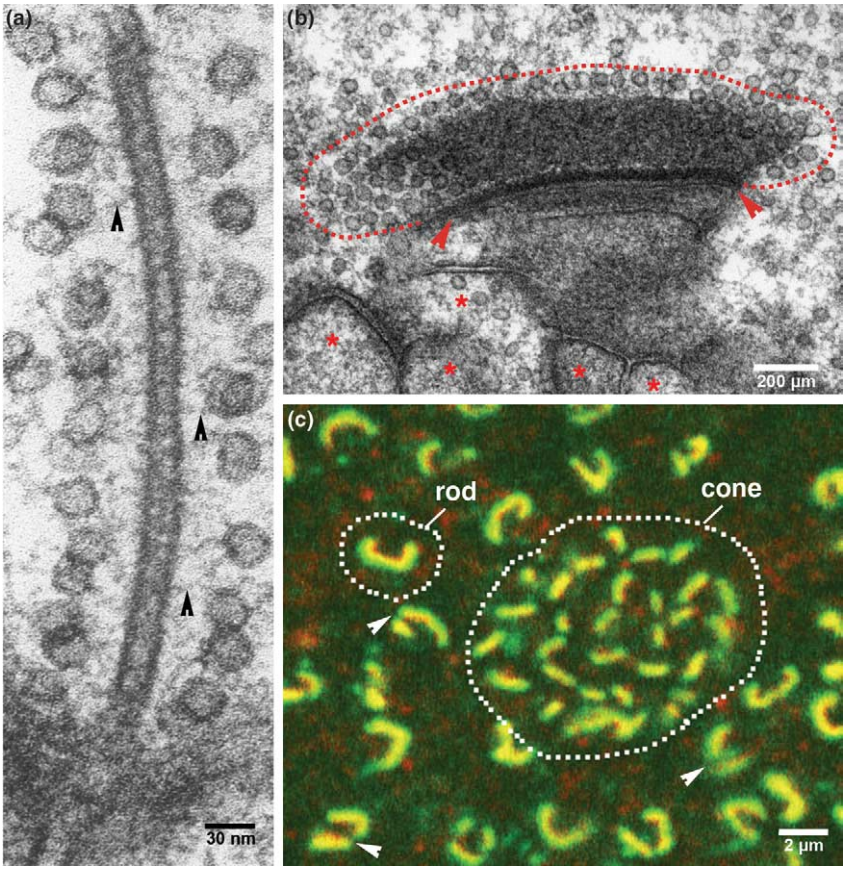

Figure 3. Structure of the ribbon synapse. **(a)** Cross-section through a ribbon in a bipolar terminal. Each vesicle is tethered to the ribbon surface by several fine filaments (arrowheads). **(b)** *En face* view of a ribbon in a cone terminal. The even spacing of vesicles is apparent. Counting vesicles enclosed by the dotted line (including both faces), ~144 vesicles are tethered and 36 are docked. Postsynaptic processes (asterisked) are numerous and located relatively far from the docking (release) sites, which are just beneath the dark ridge that anchors the ribbon to the presynaptic membrane (arrowheads). **(c)** Tangential view of photoreceptor terminals. Dotted lines outline the presynaptic terminal; green represents immunostaining for the anchoring protein Bassoon, and red represents staining for the α 1F subunit of an L-type Ca^{2+} channel. The rod terminal often contains a single, large, crescent-shaped ribbon, but commonly it 'cracks' into two separate ribbons (arrowheads) that maintain the overall crescent and serve a single invagination [102]. The cone terminal contains an array of smaller ribbons that serve separate invaginations. The number of cone ribbons increases from ~20 in the fovea to ~50 in peripheral retina [39]. All panels are from primate (macaque); (a,b) are electron micrographs; (c) merges two confocal images and is reprinted, with permission, from Ref. [23] © (2003) Springer.

synapses. Bassoon and Piccolo are both expressed at photoreceptor ribbons, but only Piccolo is expressed at bipolar ribbons [14,15].

Bassoon localizes ultrastructurally to the arciform density, which suggests a role in anchoring the ribbon (Figure 3c). Indeed, when Bassoon is functionally knocked out, most ribbons float free in the cytoplasm. Correspondingly, synaptic transmission from photoreceptor to bipolar cell is severely attenuated [15]. This provides perhaps the strongest functional evidence that an attached ribbon is crucial for normal synaptic function. If this functional knockout in hair cells has a similar effect, it would imply that even though the hair cell anchor is invisible by heavy metal staining, this important anchoring protein is present and essential.

As important as the ribbon's composition is that of the filaments tethering the vesicles to it. The filaments probably do not contain synapsin I, which clusters vesicles at conventional synapses, because this protein is absent from ribbon synapses [16]. Because the ribbon stains for kinesin, the filaments might contain a tubulin that could stride along fixed kinesin particles. However, low temperature, which depolymerizes cytoplasmic microtubules, does not affect ribbon morphology [7]. Thus, it should be kept in mind that immunostaining of the ribbon for kinesin might simply represent a fortuitous cross-reaction with a conserved epitope.

Alternatively, consider that filaments must be shed during high rates of exocytosis but do not accumulate near the ribbon. Thus, filaments probably depolymerize rapidly during exocytosis and repolymerize as vesicles are retrieved for re-release. If so, they might be actin that could step down the ribbon on a yet-to-be-discovered myosin. Against this idea, cytochalasin D reduced the filaments to some extent but by no means eliminated them [17]. Furthermore, cytochalasin D dissolved the actin cytoskeleton of bipolar terminals but did not alter exocytosis [18]; nor did latrunculin, which blocks actin polymerization [19]. Finally, Usukura and Yamada [7] state that filaments borne on the ribbon were never labeled with anti-actin antibodies.

Dystrophin, an actin-binding protein of the membrane cytoskeleton, is present in rod and cone terminals [20]. And mutations that disturb binding of dystrophin to a transmembrane protein, dystroglycan, reduce photoreceptor synaptic transmission (reduced b-wave of the electroretinogram [21]). However, these proteins do not localize to the ribbon, but rather to the lateral regions of the presynaptic membrane [22], which are sites of endocytosis (Figure 4).

Voltage-gated Ca^{2+} channels

If exocytosis is truly associated with the ribbon complex, voltage-gated Ca^{2+} channels should be expressed along the docking sites. This has now been demonstrated in several ways: (i) immunostaining for the α 1D and 1F subunits of the L-type Ca^{2+} channel precisely follows the distribution of Bassoon along the base of the ribbon [23] (Figure 3c); (ii) immunostaining for α 1D colocalizes with fluorescent dihydropropidine, an L-type channel antagonist [24]; (iii) 'hot spots' of Ca^{2+} entry in bipolar and hair cells match in number and location the ribbons identified by immunostaining for RIBEYE [25]; and (iv) Ca^{2+} hot spots colocalize with ribbons identified in the living terminal using a small peptide that binds CtBP2 [26]. The hair cell channels are also L-type [1,27], which are specialized to be fast [28]. Thus, vesicles docked along the base of the ribbon resemble the lizard neuromuscular junction, where vesicles also dock in parallel rows flanking rows of Ca^{2+} channels [29]. In both cases, the extended numbers of docking sites near Ca^{2+} channels probably serve the same function: to enlarge the releasable pool and hence the quantal content per unit time.

Quantitative aspects of presynaptic architecture

For a cell type of defined function the dimensions and shape of the ribbon are invariant. For example, the mammalian rod typically expresses a single ribbon that is always crescent-shaped and constant in size from mouse to man (Figure 3c). This ribbon provides docking sites for $\sim$130 vesicles plus a reserve depot of $\sim$640 vesicles. Such constancy makes sense for the rod synapse because its task is always the same: to transfer a binary signal, 0 or 1 photon event [30–33]. Similarly, cone terminals in a given species and retinal locus (e.g. cat central area) express a nearly constant number of ribbons (11.6 ± 0.9) and, although these differ in length from 0.2–3.5 μm, the total length per terminal is remarkably constant (9.9 ± 0.9 μm). This provides a fixed number of docking sites ($\sim$600) and depot sites ($\sim$3000) [34]. Similar numbers for the total releasable pool (3550 vesicles) based on ultrastructure are found in salamander rod [35].

That the cone docks and tethers about fivefold more vesicles than the mammalian rod suggests that ribbon size and number correlate with information rate [36]. This follows because in daylight a cone transduces 10^3–10^7 photons per integration time to produce a finely graded signal, whereas at night a rod transduces 0 or 1 photon per integration time to produce an irreducibly simple binary signal. Additional examples include the salamander rod which, being much larger than a mammalian rod, collects more information per unit time (a multi-photon, graded signal). Correspondingly, its synaptic terminal expresses about eight fairly large ribbons with releasable pools resembling those of mammalian cones [37]. Similarly, a primate foveal cone, with a narrow inner segment expresses $\sim$20 ribbons, each with $\sim$36 docking sites and 144 reserve sites (Figure 3b,c). But as the cone inner segment expands toward peripheral retina and probably captures still more information, the number of ribbons increases to $>$50 [38,39].

Hair cells also follow these general rules. Thus, the spheroidal ribbon in a frog saccular hair cell docks many vesicles ($\sim$40) and tethers nearly tenfold more ($\sim$350) [8]. Regarding total docking and tethered sites per cell, the tall hair cells of the chick cochlea (homologs of the mammalian inner hair cells) express the same average number of ribbons ($\sim$15) across the tonotopic axis. However, cells serving the high-frequency region contain much larger ribbons with more total docking and reserve sites. Furthermore, numbers of voltage-gated Ca^{2+} channels

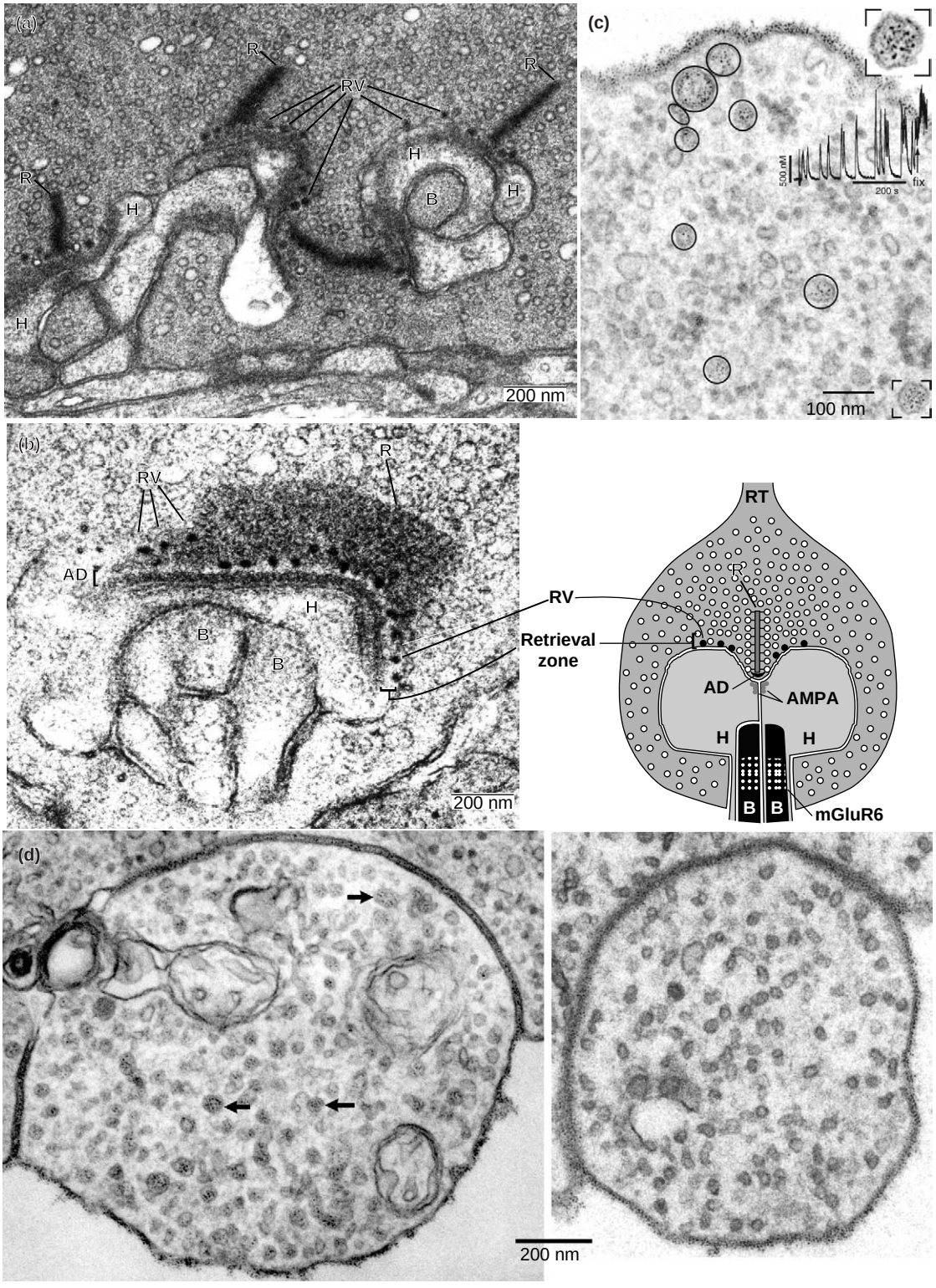

Figure 4. Sites of endocytosis (membrane retrieval). **(a)** A cone terminal. When retina is incubated in darkness for 0.5 min in microperoxidase, membrane is retrieved as ~30 nm vesicles just lateral to the active zone ('RV' indicates a retrieved vesicle). **(b)** A rod terminal (RT) from same experiment. Membrane is retrieved as vesicles along whole length of ribbon (R). Panels (a,b) are from guinea pig (M. Freed and P. Sterling, unpublished); scale bar in (b) applies to both panels. White dots on the bipolar dendrite (B) indicate the location of mGluR6 metabotropic glutamate receptors. **(c)** A goldfish bipolar terminal incubated in cationic ferritin and depolarized by high K^+ concentrations. Membrane is retrieved as large endosomes. Reproduced, with permission, from Ref. [81] © (2003) Society for Neuroscience. **(d)** Amacrine boutons attached to bipolar terminals. Left: active bouton shows numerous vesicles loaded with ferritin (arrows). Reproduced, with permission, from Ref. [81] © (2003) Society for Neuroscience. Right: silent bouton shows vesicles devoid of ferritin (G. Matthews and P. Sterling, unpublished). Additional abbreviations: AD, arciform density; AMPA, AMPA receptors; H, horizontal cell spine.

also correlate with release area over 2–3 orders of magnitude and across species [40].

Similarly, a cat inner hair cell in the 0.25 kHz region of the cochlea innervates ten afferent fibers (typically one ribbon per fiber), but one in the 10 kHz region innervates 30 afferent fibers [41,42]. Mouse apparently resembles cat, with ~25 ribbons per inner hair cell [43]. These trends – more release and more reserve sites for higher frequencies – seem consistent with the general law that a channel's information rate (bits s^{-1}) increases with temporal bandwidth (for a given signal-to-noise ratio) [36,44].

Compared with photoreceptors and hair cells, retinal bipolar cell ribbons tend to be smaller and more numerous. For example, a goldfish bipolar cell ribbon docks ~10 vesicles and tethers ~70 vesicles (D. Zenisek, G. Matthews and P. Sterling, unpublished). This terminal, a popular model for electrophysiology, expresses 40–60 ribbons [4,45]. In mammals, bipolar cells have 30–40 ribbons for slower, tonic types. For example, the rod bipolar cell expresses 30–40 ribbons (in cat, rat and mouse) [46–48]; in primates, the midget bipolar cell expresses 30–50 ribbons [49] and the S-cone ON bipolar cell expresses ~40 ribbons [50]. Transient bipolar cells express considerably more ribbons; thus the cat b_1 bipolar cell expresses 105 ribbons [51], and the apparently corresponding bipolar type in mouse expresses 120 ribbons [48]. Transient bipolar cells should transmit information at higher rates than sustained bipolar cells because they have higher temporal bandwidth and comparable signal-to-noise ratio.

Postsynaptic structure

Hair cell: one vesicle → one postsynaptic process → one spike

Ribbon synapses display diverse postsynaptic configurations. Simplest are the hair cells, where each ribbon usually supplies a single, postsynaptic bouton across a 20 nm cleft (Figure 1a). One vesicle released onto this high-resistance structure can depolarize it sufficiently to evoke an action potential [52,53], but there is clear evidence for multivesicular release from a single ribbon onto one bouton, perhaps to enhance reliability and allow an auditory afferent to follow very high temporal frequencies [53]. An auditory hair cell (in cat) can connect to 10–30 afferent boutons [41], mostly via single ribbon synapses, showing remarkable divergence. Reptilian hair cells show somewhat different patterns [54]. Thus, hair cell economics – one ribbon → one vesicle (or a few vesicles) → one afferent fiber → one action potential – are vastly simpler than for retinal neurons where divergence is always accompanied by substantial convergence [55]. For example, whereas a cone diverges to 10–20 bipolar cells, each bipolar cell receives convergent input from ~10 cones; whereas a bipolar cell diverges to several ganglion cells, each ganglion cell receives convergent input from 10–100 bipolar cells.

Photoreceptor: one vesicle → many postsynaptic processes with diverse receptors

A photoreceptor ribbon-type active zone supplies glutamate to multiple postsynaptic processes. Originating from different cell types, each expresses a characteristic type of glutamate receptor that is located at a different, but characteristic distance from the release sites. For example, the rod terminal is invaginated by a pair of horizontal cell spines that express an AMPA receptor just across the synaptic cleft, ~20 nm from release sites (Figures 1b, 2 and 5). The rod terminal is also invaginated by two or more bipolar dendrites that express a metabotropic receptor (mGluR6). The dendritic tips end several hundred nanometers away from the release sites [31,56]; however, the receptor is not expressed at the tips but slightly down the shaft near the mouth of the invagination [57]. Consequently, the diffusion distance from vesicle release sites to these receptors is several hundreds of nanometers. Furthermore, the release sites are aligned along the concave edge of the rod ribbon's stereotypical crescent [31]; thus the release sites in effect arch above the receptor sites. This tends to equalize the distance from all release sites to these glutamate receptors and thus minimize differences in spatiotemporal glutamate concentration between vesicles released from different sites along the ribbon [32].

The cone ribbon synapse exhibits an even richer variety of postsynaptic structures [38,39,58,59]. First, resembling the rod terminal, there is a 'triad', comprising two horizontal cell spines near the release sites, plus one or several invaginating bipolar dendrites with tips far from the release sites. The horizontal cell spines express AMPA receptors [38], and the bipolar dendrites express mGluR6, also not at the tip but several hundred nanometers down the shaft [57]. Second, the cone terminal's basal surface, except for the invaginations, is densely studded with the dendritic tips of various types of bipolar cell, each located at a characteristic distance from the triad [60,61]. These express a panoply of ionotropic glutamate receptors whose properties can be matched to the different distances. Thus, immunostaining shows puncta for the GluR1 subunit (AMPA type) nearest to the triad, and puncta for GluR5 and GluR6/7 subunits (kainate types) further from the triad [38,58].

These arrangements might explain how bipolar types come to express different kinetics and pharmacology. Thus, one type shows large, fast currents with AMPA pharmacology, and rapid recovery from desensitization, whereas two other types show smaller, slower currents with kainate pharmacology and slower recovery [62,63]. It is anticipated that cells with the fast receptor kinetics will correspond to those with AMPA immunostaining whose dendrites end nearest the triads, and that cells with slower kinetics will correspond to the kainate staining and be farther away. Even so, all bipolar dendrites, including those expressing mGluR6 and subunits of AMPA and kainate receptors, are 10–50 fold further from release sites than is typical for a conventional synapse (Figures 4,5).

Finally, ~1000–2000 nm beneath the basal surface of the cone terminal, pairs of horizontal cell processes exhibit small electron-dense patches. These prove to be ionotropic glutamate receptors, containing both AMPA and kainate subunits [38,58]. Glutamate released from the ribbon might reach these receptors, despite the immense distance, because glial processes, whose glutamate transporters

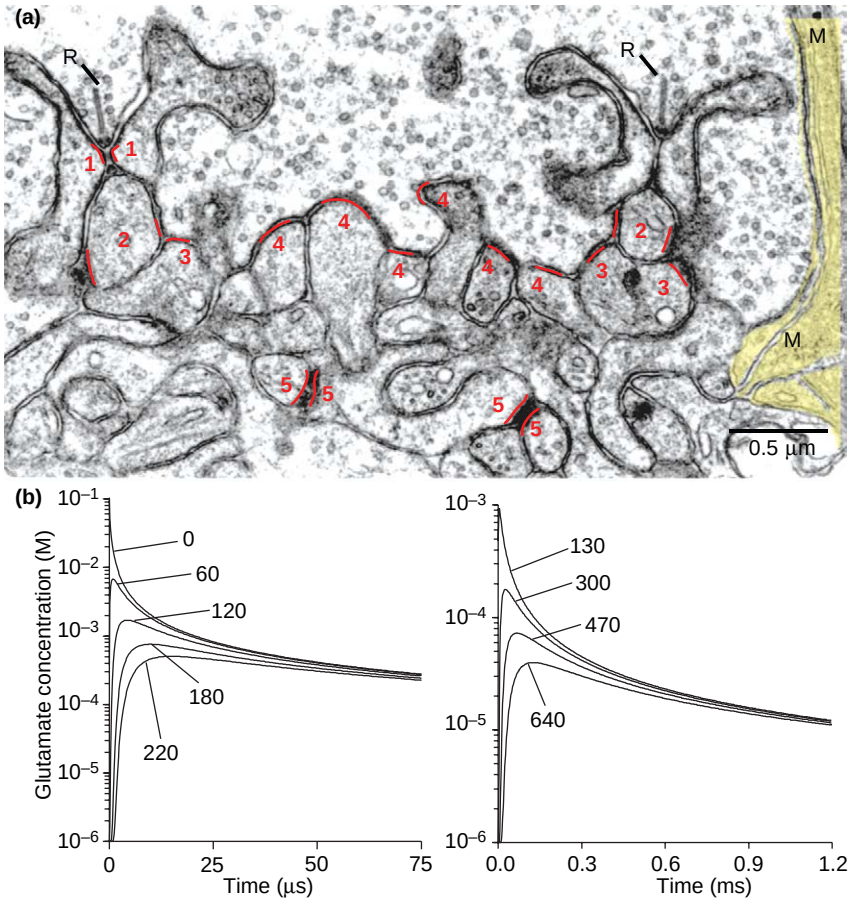

Figure 5. Architecture of cone synapses allows each vesicle to affect many postsynaptic processes ('engineered spillover'). **(a)** Vertical section through the base of a macaque cone terminal showing two ribbons (R). The numbers signify postsynaptic glutamate receptors near the release sites (1) and progressively further away (2–5). Each location might express a unique subset of glutamate receptors (red lines) optimized for its most likely spatiotemporal concentration [38]. Müller cell (M) wrappings separate adjacent terminals but avoid the region beneath the terminal, thus allowing multivesicular pooling of glutamate beneath each terminal but restricting interaction between terminals [64]. **(b)** Glutamate concentration rises to high levels and falls quickly near the release site. With increasing distance, diffusion reduces the peak concentration and slows its rise and decay. Such patterns might be matched to the binding properties of the receptors at the locations in (a). These calculations are based on geometry of the rod terminal. Modified, with permission, from Ref. [32].

would rapidly remove glutamate from the cleft, separate neighboring cone terminals but are excluded from the region beneath the terminal [64] (Figure 5a). Of course, individual glutamate quanta diffusing over this great distance will merge in the extracellular cleft and could cause slow modulations in extracellular glutamate to transmit low temporal frequencies to the horizontal cell dendrites.

In summary, each vesicle released from a cone synaptic ribbon contributes glutamate to postsynaptic processes at five, progressively more distant locations. The spatiotemporal profile of the glutamate quantum will be progressively smeared [32] (Figure 3b), but specific combinations of glutamate receptors at each location could optimize their binding kinetics to the characteristic spatiotemporal concentration. The nearer, faster receptors would detect individual quanta, but the farther, slower receptors would allow spatiotemporal integration of multiple quanta and thus cooperation between adjacent ribbons. This arrangement would allow each vesicle to contribute information at different temporal bandwidths to different postsynaptic cell types and thus extract the most information from each vesicle.

Bipolar cell: one vesicle → two processes with different receptors

The bipolar ribbon is usually presynaptic to a pair of processes (dyad). The glutamate receptors are always fairly near the release site and symmetrically placed, so each postsynaptic process sees the identical spatiotemporal profile of glutamate. However, the two processes commonly express different receptors: ganglion cell dendrites preferentially express AMPA and NMDA receptors, whereas amacrine processes express kainate receptors and the orphan receptor subunits δ1/δ2 [65]. It is interesting that geometry of the bipolar synapse is far simpler than that of the photoreceptor. Perhaps this occurs because filtering at the first synapse gives each bipolar type a narrower range of frequencies to transfer at its output. However, it is far from clear why the design calls for two postsynaptic processes rather than three or more.

Exocytosis at ribbon synapses

Exocytosis at the bipolar ribbon synapse has been observed directly. Using total internal reflection microscopy, vesicles labeled by the dye FM1-43 are seen to pause at the membrane and then, upon opening of Ca^{2+} channels, to

release all the dye promptly [66]. Destaining occurs within milliseconds, consistent with full fusion [67]. This rules out release by a kiss-and-run process, which would require the dye to dissociate from the lipid phase and exit via an aqueous pore, requiring seconds. Full collapse of the vesicle into the plasma membrane is further supported by interference reflection microscopy [68].

The bipolar cell active zone can release neurotransmitter continuously for hundreds of milliseconds during strong stimulation. This release exhibits two kinetically distinct components: a small fast pool (~20% of the total) is released in ~1 ms, and a large sustained pool (~80%) is released over several hundred milliseconds [69–71]. The fast pool matches the number of vesicles docked at the base of the ribbon, and the sustained pool matches the number of vesicles tethered to the ribbon in higher rows, more distant from the plasma membrane [45]. Similarly, release at the salamander rod synapse also exhibits transient and sustained components, on timescales of milliseconds and hundreds of milliseconds, and the size of the releasable pool matches the number of vesicles tethered to the ribbon [35]. So, the large size of the sustained component is what functionally distinguishes ribbon-type active zones from conventional active zones, where sustained release is typically minor.

The neat correspondence between the pool of tethered vesicles and the pool for sustained release in both rods and bipolar cells suggests that the ribbon might serve as a platform where vesicles can be primed to allow sustained release. However, if vesicles can fuse at sites other than ribbons during sustained release [66], the match between the structurally tethered pool and the functional pool could be spurious. Because Ca^{2+} channels concentrate at ribbons [23,25–27,72,73], Ca^{2+}-triggered exocytosis is expected to occur preferentially at ribbons, where postsynaptic receptors are also concentrated (Figure 1c). Matching this expectation, release at the rod synapse is quantitatively similar whether measured with postsynaptic currents (reflecting focal release at the ribbon) or with presynaptic capacitance changes (potentially reflecting both focal and ectopic release) [35]. Yet the equivalence of tethered and releasable vesicles does not extend to the hair cell ribbon, where the sustained pool proves to be ~6–8 times larger than the number of vesicles tethered to the spheroidal ribbons [74]. This might suggest that the match in photoreceptor and bipolar cells is pure coincidence – or that hair cell vesicles can be primed before attaching to the ribbon – or that priming reactions are faster in hair cells, allowing vesicles to cycle more rapidly across the ribbon [75].

How might the primed vesicles in higher rows on the ribbon release their neurotransmitter during sustained stimulation? One possibility is that the filaments connecting vesicles to the ribbon constitute a molecular motor that transports vesicles in successive waves to the base, where they then fuse with the plasma membrane. However, any such motor must not require ATP hydrolysis, because the full complement of vesicles can be released with normal kinetics in the presence of ATPγS, which does not support ATP-dependent motors such as kinesin or myosin [76]. If the functional pool does correspond to the tethered pool (despite the preceding caveats), it follows that all the vesicles on the ribbon have undergone the essential priming reactions that require ATP hydrolysis. Conceivably, vesicles on the face of the ribbon might dock with each other, allowing a wave of compound fusion to sweep up the ribbon during sustained transmitter release [5,8,77].

Once depleted, the bipolar cell's releasable pool requires several seconds to refill [78]. Refilling is severely retarded when ATP hydrolysis is inhibited [77,79], which suggests a central role for ATP-dependent priming in functional recovery of this releasable pool. Thus the bipolar ribbon might provide a platform to prime vesicles and then hold the newly fusion-competent vesicles near to release sites. By contrast, the hair cell's releasable pool refills much faster (<200 ms) [75], suggesting that vesicles in the hair cell can be primed in the cytoplasm, before tethering to the ribbon.

Endocytosis

The large amount of exocytosis during sustained transmitter release requires equally high-capacity endocytosis to retrieve the added membrane. In cone photoreceptors, fused membrane is directly recycled into small synaptic vesicles, without intermediate pooling into endosomes [80] (Figure 4a,b). The recycled vesicles are mobile and, diffusing as fast as similarly sized microspheres, rapidly replenish the releasable pool [80]. Surprisingly, bipolar cells rely on a different mechanism for rapid retrieval, in which membrane is endocytosed in large bites that only later give rise to recycled synaptic vesicles [19,81] (Figure 4c). Unlike cones, where newly recycled vesicles rapidly appear in the pool tethered to ribbons, recycled vesicles make up only ~10% of the vesicles on bipolar cell ribbons, even after >10 min of activity [80]. Thus, the bipolar cell relies on its large reserve of synaptic vesicles to replenish the releasable pool, whereas cone photoreceptors evidently have no reserve pool and rely instead on rapid recycling. In this regard, the cone ribbon synapse resembles the conventional amacrine cell synapse, where extensive labeling of recycled synaptic vesicles was observed, without significant labeling in larger endosomes [81] (Figure 1d). Like bipolar cells, hair cells exhibit large numbers of endosomes and membrane invaginations after stimulation [8], which suggests that hair cells and bipolar cells might share a common mechanism of membrane retrieval.

Ca^{2+} sensitivity

Exocytosis at ribbon synapses, as for all chemical synapses, is regulated by Ca^{2+}. But the Ca^{2+}-dependence of release varies. Hair cell ribbon synapses exhibit a steep dependence on Ca^{2+} concentration ($[Ca^{2+}]$), with a Hill coefficient of 5 [82]. Bipolar cells also exhibit a steep dependence on $[Ca^{2+}]$ [83]. The physiological rate of vesicle release at bipolar terminals is likely to require 20–50 μM free Ca^{2+} [84], whereas a slower form of membrane turnover is stimulated by lower Ca^{2+} levels [85,86]. By contrast, exocytosis at the photoreceptor synapse is less steeply dependent on $[Ca^{2+}]$ and is stimulated by much lower levels of free Ca^{2+} (~1 μM) [35]. The upshot is that transmitter release at the photoreceptor synapse is approximately linearly related

to Ca^{2+} current, a feature that might help expand the dynamic range of a cell whose physiological range of membrane potential (−40 to −60 mV) spans the negative tail of the activation range for Ca^{2+} channels.

Presynaptic regulation

Exocytosis at ribbon synapses is regulated by diverse feedback mechanisms. (i) Horizontal cell spines that invaginate cone terminals might exert their negative effect by injecting an ephaptic current through a hemi-junction [87]. (ii) Horizontal cells release GABA, which might feedback to $GABA_A$ receptors [88]. (iii) Glutamate released at the photoreceptor activates a voltage-dependent glutamate transporter that drives a concentration-dependent Cl^- current [89,90]. (iv) Photoreceptor and bipolar terminals express metabotropic glutamate receptors that regulate voltage-gated Ca^{2+} channels [91,92]. (v) synaptic vesicles release protons that inhibit Ca^{2+} channels and thus tend to locally inhibit further release. This occurs both at the cone [93] and the bipolar [94] terminals. Such proton-mediated inhibition, by creating a local refractory period for release, might help ensure that all regions of the extended active zone are used equally. (vi) GABA from amacrine processes can feedback onto the bipolar terminal to limit and synchronize release [92,95,96]. (vii) Photoreceptor ribbons can change shape and size, apparently in response to changes in illumination and with time of day [97]. How these shifts affect the rates of exocytosis remains to be investigated.

Release rates during natural stimulation

Measurements of release kinetics and pool size generally use a cell voltage-clamped in isolation or in a tissue slice. But a few studies have measured rates during natural stimulation of an intact circuit. Analyzing synaptic noise in a turtle OFF bipolar cell suggested ~9200 transmitter-related events per second [98]. Assuming that each represents one vesicle, and estimating the number of contributing active zones, one active zone can apparently sustain release at ~20 vesicles s^{-1}. Noise analysis of mouse cone bipolar cells gave a similar result [99].

Both studies found that bright light completely suppresses noise in the bipolar cell, suggesting that light can strongly suppress release. This is confirmed by experiments with the dye FM1-43, which once loaded into vesicles by endocytosis [80] can be retained completely by steady illumination, and then discharged nearly completely upon return to darkness. The maximum release rate calculated from this study is ~300 vesicles s^{-1} per cone (Kramer *et al.*, unpublished). At the mammalian rod synapse the sustained rate has not been measured, but calculations suggest that to transfer a single photon event reliably, it should release ~100 vesicles s^{-1} [32,33].

Noise analyses of ganglion cells in the intact retina support the idea that different bipolar types release quanta at different rates. Thus, the rate needed to evoke a just-maximal sustained response in a brisk-transient ganglion cell is ~3700 quanta s^{-1}, corresponding per ribbon synapse to ~1.7 quanta s^{-1}. Transient release at this ribbon synapse could rise as high as 17 quanta s^{-1} [100]. The maximal sustained response of a brisk-sustained ganglion cell can reach 45 000 quanta s^{-1} and depends on two different types of bipolar cell, whose synapses appear to release at high sustained rates, at >20 quanta s^{-1} [101]. However, for stimuli in a more natural range of contrasts and frequencies, the rates are far lower, at ~120 quanta s^{-1} for the ganglion cell (M. Freed, pers. commun.).

Concluding remarks

The idea that the ribbon assists high rates of sustained exocytosis now seems well supported by combined analyses of structure and function. The variations in ribbon morphology and ribbon number across cell types suggest that this organelle is further tailored very specifically to deliver particular rates under particular conditions. To test this will require comparing morphology with careful measurements of release under natural conditions. At least as interesting, and possibly more challenging, will be to discover whether vesicles actually move on the ribbon, and how retrieved vesicles return to the release sites. The answers might require stopping the action, perhaps by rapid freeze followed by electron microscopy, or by further studies with total internal reflection fluorescence (TIRF) microscopy to follow vesicles in real time.

Acknowledgements

We thank Thomas Parsons for comments on the manuscript, Sharron Fina for preparing it, and Judith McLean for contributing Figures 1 and 2. Supported by National Eye Institute grants, EY00828, EY08124 (P.S.) and EY03821 (G.M.).

References

1 Fuchs, P.A. *et al*. (2003) The afferent synapse of cochlear hair cells. *Curr. Opin. Neurobiol.* 13, 452–458
2 Sejnowski, T.J. and Yodlowski, M.L. (1982) A freeze-fracture study of the skate electroreceptor. *J. Neurocytol.* 11, 897–912
3 Lenzi, D. and von Gersdorff, H. (2001) Structure suggests function: the case for synaptic ribbons as exocytotic nanomachines. *Bioessays* 23, 831–840
4 Lagnado, L. (2003) Ribbon synapses. *Curr. Biol.* 13, R631
5 Parsons, T. and Sterling, P. (2003) Synaptic ribbon: conveyor belt or safety belt? *Neuron* 37, 379–382
6 von Gersdorff, H. and Matthews, G. (1999) Electrophysiology of synaptic vesicle cycling. *Annu. Rev. Physiol.* 61, 725–752
7 Usukura, J. and Yamada, E. (1987) Ultrastructure of the synaptic ribbons in photoreceptor cells of *Rana catesbeiana* revealed by freeze-etching and freeze-substitution. *Cell Tissue Res.* 247, 483–488
8 Lenzi, D. *et al*. (2002) Depolarization redistributes synaptic membrane and creates a gradient of vesicles on the synaptic body at a ribbon synapse. *Neuron* 36, 649–659
9 Lenzi, D. *et al*. (1999) Synaptic vesicle populations in saccular hair cells reconstructed by electron tomography. *J. Neurosci.* 19, 119–132
10 Wang, Y. *et al*. (1997) Rim is a putative Rab3 effector in regulation synaptic-vesicle fusion. *Nature* 388, 593–598
11 Schmitz, F. *et al*. (1996) Purification of synaptic ribbons, structural components of the photoreceptor active zone complex. *J. Neurosci.* 16, 7109–7116
12 Schmitz, F. *et al*. (2000) RIBEYE, a component of synaptic ribbons. *Neuron* 28, 857–872
13 Muresan, V. *et al*. (1999) The kinesin motor KIF3A is a component of the presynaptic ribbon in vertebrate photoreceptors. *J. Neurosci.* 19, 1027–1037
14 Brandstätter, J.H. *et al*. (1999) Differential expression of the presynaptic cytomatrix protein bassoon among ribbon synapses in the mammalian retina. *Eur. J. Neurosci.* 11, 3683–3693
15 Dick, O. *et al*. (2003) The presynaptic active zone protein bassoon is essential for photoreceptor ribbon synapse formation in the retina. *Neuron* 37, 775–786

16 Mandell, J.W. *et al*. (1990) Synapsins in the vertebrate retina: absence from ribbon synapses and heterogeneous distribution among conventional synapses. *Neuron* 5, 19–33
17 Peschke, E. *et al*. (1996) Morphometry of pineal synaptic ribbon profile numbers after cytochalasin D treatment. *Acta Anat. (Basel)* 156, 94–98
18 Job, C. and Lagnado, L. (1998) Calcium and protein kinase C regulate the actin cytoskeleton in the synaptic terminal of retinal bipolar cells. *J. Cell Biol.* 143, 1661–1672
19 Holt, M. *et al*. (2004) High mobility of vesicles supports continuous exocytosis at a ribbon synapse. *Curr. Biol.* 14, 173–183
20 Ueda, H. *et al*. (1995) Dystrophin localization at presynapse in rat retina revealed by immunoelectron microscopy. *Invest. Ophthalmol. Vis. Sci.* 36, 2318–2322
21 Lenk, U. *et al*. (1996) A cysteine 3340 substitution in the dystroglycan-binding domain of dystrophin associated with Duchenne muscular dystrophy, mental retardation and absence of the ERG b-wave. *Hum. Mol. Genet.* 5, 973–975
22 Schmitz, F. and Drenckhahn, D. (1997) Localization of dystrophin and β-dystroglycan in bovine retinal photoreceptor processes extending into the postsynaptic dendritic complex. *Histochem. Cell Biol.* 108, 249–255
23 Wässle, H. *et al.* (2003) The cone pedicle, the first synapse in the retina. In *The Neural Basis of Early Vision*, pp. 19–38, Springer Verlag, Tokyo
24 Nachman-Clewner, M. *et al*. (1999) L-type calcium channels in the photoreceptor ribbon synapse: localization and role in plasticity. *J. Comp. Neurol.* 415, 1–16
25 Zenisek, D. *et al*. (2003) Imaging calcium entry sites and ribbon structures in two presynaptic cells. *J. Neurosci.* 23, 2538–2548
26 Zenisek, D. *et al.* (2004) Visualizing synaptic ribbons in the living cell. *J. Neurosci.* (in press)
27 Zidanic, M. and Fuchs, P.A. (1995) Kinetic analysis of barium currents in chick cochlear hair cells. *Biophys. J.* 68, 1323–1336
28 Mennerick, S. and Matthews, G. (1998) Rapid calcium-current kinetics in synaptic terminals of goldfish retinal bipolar neurons. *Vis. Neurosci.* 15, 1051–1056
29 Walrond, J.P. and Reese, T.S. (1985) Structure of axon terminals and active zones at synapses on lizard twitch and tonic muscle fibers. *J. Neurosci.* 5, 1118–1131
30 Field, G.D. and Rieke, F. (2002) Nonlinear signal transfer from mouse rods to bipolar cells and implications for visual sensitivity. *Neuron* 34, 773–785
31 Rao-Mirotznik, R. *et al*. (1995) Mammalian rod terminal: Architecture of a binary synapse. *Neuron* 14, 561–569
32 Rao-Mirotznik, R. *et al*. (1998) Transmitter concentration at a three-dimensional synapse. *J. Neurophysiol.* 80, 3163–3172
33 van Rossum, M.C.W. and Smith, R.G. (1998) Noise removal at the rod synapse of mammalian retina. *Vis. Neurosci.* 15, 809–821
34 Sterling, P. (2004) How retinal circuits optimize the transfer of visual information. In *The Visual Neurosciences* (Chalupa, L.M. and Werner, J.S., eds), pp. 243–268, MIT Press
35 Thoreson, W.B. *et al*. (2004) A highly Ca^{2+}-sensitive pool of vesicles contributes to linearity at the rod photoreceptor ribbon synapse. *Neuron* 42, 595–605
36 de Ruyter van Steveninck, R. and Laughlin, S.B. (1996) The rate of information transfer at graded-potential synapses. *Nature* 379, 642–645
37 Townes-Anderson, E. *et al*. (1985) Rod cells dissociated from mature salamander retina: ultrastructure and uptake of horseradish peroxidase. *J. Cell Biol.* 100, 175–188
38 Haverkamp, S. *et al*. (2000) The cone pedicle, a complex synapse in the retina. *Neuron* 27, 85–95
39 Haverkamp, S. *et al*. (2001) The synaptic architecture of AMPA receptors at the cone pedicle of the primate retina. *J. Neurosci.* 21, 2488–2500
40 Martinez-Dunst, C. *et al*. (1997) Release sites and calcium channels in hair cells of the chick's cochlea. *J. Neurosci.* 17, 9133–9144
41 Liberman, M.C. (1982) Single-neuron labeling in the cat auditory nerve. *Science* 216, 1239–1241
42 Liberman, M.C. *et al*. (1990) Afferent and efferent innervation of the cat cochlea: quantitative analysis with light and electron microscopy. *J. Comp. Neurol.* 301, 443–460
43 Moser, T. and Beutner, D. (2000) Kinetics of exocytosis and endocytosis at the cochlear inner hair cell afferent synapse of the mouse. *Proc. Natl. Acad. Sci. U. S. A.* 97, 883–888
44 Rieke, F. *et al.* (1999) Spikes: exploring the neural code. (Sejnowski, T.J. and Poggio, T.A., eds), MIT Press
45 von Gersdorff, H. *et al*. (1996) Evidence that vesicles on the synaptic ribbon of retinal bipolar neurons can be rapidly released. *Neuron* 16, 1221–1227
46 McGuire, B.A. *et al*. (1984) Microcircuitry of bipolar cells in cat retina. *J. Neurosci.* 4, 2920–2938
47 Singer, J.H. *et al*. (2004) Coordinated multivesicular release at a mammalian ribbon synapse. *Nat. Neurosci.* 7, 826–833
48 Tsukamoto, Y. *et al*. (2001) Microcircuits for night vision in mouse retina. *J. Neurosci.* 21, 8616–8623
49 Calkins, D.J. *et al*. (1994) M and L cones in *Macaque* fovea connect to midget ganglion cells via different numbers of excitatory synapses. *Nature* 371, 70–72
50 Calkins, D.J. *et al*. (1998) Microcircuitry and mosaic of a blue/yellow ganglion cell in the primate retina. *J. Neurosci.* 18, 3373–3385
51 Cohen, E. and Sterling, P. (1990) Demonstration of cell types among cone bipolar neurons of cat retina. *Philos. Trans. R. Soc. Lond. Biol. Sci.* 338, 305–321
52 Siegel, J.H. (1992) Spontaneous synaptic potentials from afferent terminals in the guinea pig cochlea. *Hear. Res.* 59, 85–92
53 Glowatzki, E. and Fuchs, P.A. (2002) Transmitter release at the hair cell ribbon synapse. *Nat. Neurosci.* 5, 147–154
54 Sneary, M.G. (1988) Auditory receptor of the red-eared turtle: II. Afferent and efferent synapses and innervation patterns. *J. Comp. Neurol.* 276, 588–606
55 Sterling, P. *et al*. (1988) Architecture of the rod and cone circuits to the on-beta ganglion cell. *J. Neurosci.* 8, 623–642
56 Migdale, K. *et al*. (2003) Two ribbon synaptic units in rod photoreceptors of macaque, human, and cat. *J. Comp. Neurol.* 455, 100–112
57 Vardi, N. *et al*. (2000) Localization of mGluR6 to dendrites of ON bipolar cells in primate retina. *J. Comp. Neurol.* 423, 402–412
58 Haverkamp, S. *et al*. (2001) Localization of kainate receptors at the cone pedicles of the primate retina. *J. Comp. Neurol.* 436, 471–486
59 Haverkamp, S. and Wässle, H. (2000) Immunocytochemical analysis of the mouse retina. *J. Comp. Neurol.* 424, 1–23
60 Hopkins, J.M. and Boycott, B. (1997) The cone synapses of cone bipolar cells of primate retina. *J. Neurocytol.* 26, 313–325
61 Calkins, D.J. *et al*. (1996) Foveal cones form basal as well as invaginating contacts with diffuse ON bipolar cells. *Vision Res.* 36, 3373–3381
62 DeVries, S.H. (2000) Bipolar cells use kainate and AMPA receptors to filter visual information into separate channels. *Neuron* 28, 847–856
63 DeVries, S.H. and Schwartz, E.A. (1999) Kainate receptors mediate synaptic transmission between cones and 'Off' bipolar cells in a mammalian retina. *Nature* 397, 157–160
64 Burris, C. *et al*. (2002) How Müller glial cells in macaque fovea coat and isolate the synaptic terminals of cone photoreceptors. *J. Comp. Neurol.* 453, 100–111
65 Grünert, U. *et al*. (2002) Synaptic distribution of ionotropic glutamate receptors in the inner plexiform layer of the primate retina. *J. Comp. Neurol.* 447, 138–151
66 Zenisek, D. *et al*. (2000) Transport, capture and exocytosis of single synaptic vesicles at active zones. *Nature* 406, 849–854
67 Zenisek, D. *et al*. (2002) A membrane marker leaves synaptic vesicles in milliseconds after exocytosis in retinal bipolar cells. *Neuron* 35, 1085–1097
68 Llobet, A. *et al*. (2003) Real-time measurement of exocytosis and endocytosis using interference of light. *Neuron* 40, 1075–1086
69 Mennerick, S. and Matthews, G. (1996) Ultrafast exocytosis elicited by calcium current in synaptic terminals of retinal bipolar cells. *Neuron* 17, 1241–1249
70 von Gersdorff, H. *et al*. (1998) Submillisecond kinetics of glutamate release from a sensory synapse. *Neuron* 21, 1177–1188
71 Singer, J.H. and Diamond, J.S. (2003) Sustained Ca^{2+} entry elicits transient postsynaptic currents at a retinal ribbon synapse. *J. Neurosci.* 23, 10923–10933

72 Issa, N.P. and Hudspeth, A.J. (1994) Clustering of Ca^{2+} channels and Ca^{2+}-activated K^+ channels at fluorescently labeled presynaptic active zones of hair cells. *Proc. Natl. Acad. Sci. U. S. A.* 91, 7578–7582
73 Llobet, A. *et al*. (2003) Exocytosis at the ribbon synapse of retinal bipolar cells studied in patches of presynaptic membrane. *J. Neurosci.* 23, 2706–2714
74 Eisen, M.D. *et al*. (2004) Large releasable pool of synaptic vesicles in chick cochlear hair cells. *J. Neurophysiol.* 91, 2422–2428
75 Spassová, M. *et al.* Evidence that rapid vesicle replenishment of the synaptic ribbon mediates recovery from short-term adaptation at the hair cell afferent synapse. *J. Assoc. Res. Otolaryngol.* (in press)
76 Heidelberger, R. *et al*. (2002) Roles of ATP in depletion and replenishment of the releasable pool of synaptic vesicles. *J. Neurophysiol.* 88, 98–106
77 Heidelberger, R. (1998) Adenosine triphosphate and the late steps in calcium-dependent exocytosis at a ribbon synapse. *J. Gen. Physiol.* 111, 225–241
78 von Gersdorff, H. and Matthews, G. (1997) Depletion and replenishment of vesicle pools at a ribbon-type synaptic terminal. *J. Neurosci.* 17, 1919–1927
79 Heidelberger, R. *et al*. (2003) Differential distribution of synaptotagmin immunoreactivity among synapses in the goldfish, salamander, and mouse retina. *Vis. Neurosci.* 20, 37–49
80 Rea, R. *et al*. (2004) Streamlined synaptic vesicle cycle in cone photoreceptor terminals. *Neuron* 41, 755–766
81 Paillart, C. *et al*. (2003) Endocytosis and vesicle recycling at a ribbon synapse. *J. Neurosci.* 23, 4092–4099
82 Beutner, D. *et al*. (2001) Calcium dependence of exocytosis and endocytosis at the cochlear inner hair cell afferent synapse. *Neuron* 29, 681–690
83 Heidelberger, R. *et al*. (1994) Calcium dependence of the rate of exocytosis in a synaptic terminal. *Nature* 371, 513–515
84 Heidelberger, R. (2001) ATP is required at an early step in compensatory endocytosis in synaptic terminals. *J. Neurosci.* 21, 6467–6474
85 Lagnado, L. *et al*. (1996) Continuous vesicle cycling in the synaptic terminal of retinal bipolar cells. *Neuron* 17, 957–967
86 Rouze, N.C. and Schwartz, E.A. (1998) Continuous and transient vesicle cycling at a ribbon synapse. *J. Neurosci.* 18, 8614–8624
87 Kamermans, M. *et al*. (2001) Hemichannel-mediated inhibition in the outer retina. *Science* 292, 1178–1180
88 Pattnaik, B. *et al*. (2000) $GABA_C$ receptors are localized with microtubule-associated protein 1B in mammalian cone photoreceptors. *J. Neurosci.* 20, 6789–6796
89 Grant, G.B. and Werblin, F.S. (1996) A glutamate-elicited chloride current with transporter-like properties in rod photoreceptors of the tiger salamander. *Vis. Neurosci.* 13, 135–144
90 Roska, B. *et al*. (1998) Voltage-dependent uptake is a major determinant of glutamate concentration at the cone synapse: an analytical study. *J. Neurophysiol.* 80, 1951–1960
91 Awatramani, G.B. and Slaughter, M.M. (2001) Intensity-dependent, rapid activation of presynaptic metabotropic glutamate receptors at a central synapse. *J. Neurosci.* 21, 741–749
92 Freed, M.A. *et al*. (2003) Timing of quantal release from the retinal bipolar terminal is regulated by a feedback circuit. *Neuron* 38, 89–101
93 DeVries, S.H. (2001) Exocytosed protons feedback to suppress the Ca^{2+} current in mammalian cone photoreceptors. *Neuron* 32, 1107–1117
94 Palmer, M.J. *et al*. (2003) Synaptic cleft acidification and modulation of short-term depression by exocytosed protons in retinal bipolar cells. *J. Neurosci.* 23, 11332–11341
95 Euler, T. and Masland, R.H. (2000) Light-evoked responses of bipolar cells in a mammalian retina. *J. Neurophysiol.* 83, 1817–1829
96 Shields, C.R. *et al*. (2000) Distinct ionotropic GABA receptors mediate presynaptic and postsynaptic inhibition in retinal bipolar cells. *J. Neurosci.* 20, 2673–2682
97 Spiwoks-Becker, I. *et al*. (2004) Mouse photoreceptor synaptic ribbons lose and regain material in response to illumination changes. *Eur. J. Neurosci.* 19, 1559–1571
98 Ashmore, J.F. and Copenhagen, D. (1983) An analysis of transmission from cones to hyperpolarizing bipolar cells in the retina of the turtle. *J. Physiol.* 340, 569–597
99 Berntson, A. and Taylor, W.R. (2003) The unitary event amplitude of mouse retinal on-cone bipolar cells. *Vis. Neurosci.* 20, 621–626
100 Freed, M.A. (2000) Rate of quantal excitation to a retinal ganglion cell evoked by sensory input. *J. Neurophysiol.* 83, 2956–2966
101 Freed, M.A. (2000) Parallel cone bipolar pathways to ganglion cell use different rates and amplitudes of quantal excitation. *J. Neurosci.* 20, 3956–3963
102 Burris, C. *et al*. (2002) How Müller glial cells in macaque fovea coat and isolate the synaptic terminals of cone photoreceptors. *J. Comp. Neurol.* 453, 100–111

2005 Wall Planner – correction

In the 2005 wall planner that accompanied the December issue of *TINS*, the title of the February 2005 issue of *Current Opinion in Neurobiology* should read 'Development' and the title of the April 2005 issue should read 'Cognitive neuroscience'. We apologize to our readers and to the *CONB* authors for this error.